STRUCTURAL CONTROL AND HEALTH MONITORING
Struct. Control Health Monit. 2008; **15**:237–264
Published online 1 February 2008 in Wiley InterScience
(www.interscience.wiley.com) DOI: 10.1002/stc.241

Cable–deck dynamic interactions at the International Guadiana Bridge: On-site measurements and finite element modelling

Elsa Caetano[1], Alvaro Cunha[1], Vincenzo Gattulli[2,*,†] and Marco Lepidi[2]

[1] *Faculty of Engineering of Porto (FEUP), Porto, Portugal*
[2] *Dipartimento di Ingegneria delle Strutture, delle Acque e del Terreno, University of L'Aquila, Monteluco di Roio, Italy*

SUMMARY

The International Guadiana Bridge is a cable-stayed bridge crossing the Guadiana River, which marks the southern border between Portugal and Spain. The bridge has a central span of 324 m and a total length of 666 m and was open to traffic in 1991. Despite the globally satisfying behaviour under the common environmental loads, which largely ensures the bridge serviceability, frequent episodes of cable vibration have been observed since completion of the construction. In this paper, the bridge modal properties and dynamic behaviour, identified from repeated campaigns of vibration data acquisitions, are compared with the response of a three-dimensional finite element model, including the description of the cable transversal motion. The model, after minor updating, furnishes a realistic reproduction of the current bridge dynamic behaviour. Then different possible justifications of the local vibrations are evaluated, briefly scanning the known sources of large amplitude cable oscillations both in the linear and the nonlinear field. In particular, the occurrence of different internal resonance conditions is deeply discussed, in order to verify whether the experimental observations could be really justified by a cable–deck dynamic interaction mechanism. Among different possibilities, a beating phenomenon between two resonant modes, amplified by the lower damping and inertial characteristics of the local mode with respect to the global one, is selected as the most critical cable excitation source. Since the cable vibrations are proved to persist for different wind conditions, the heavy traffic load on the bridge deck is investigated as one possible source of the global mode direct excitation. On this respect, the model response to random load and moving forces acting on the bridge deck is numerically evaluated evidencing how some particular features of the real bridge behaviour can be qualitatively reproduced. Copyright © 2008 John Wiley & Sons, Ltd.

KEY WORDS: cable-stayed bridge; cable vibration; ambient vibration measurements; finite element modelling; dynamic interaction; traffic load

*Correspondence to: Vincenzo Gattulli, Dipartimento di Ingegneria delle Strutture, delle Acque e del Terreno, University of L'Aquila, Monteluco di Roio, Italy.
† E-mail: gattulli@ing.univaq.it

Contract/grant sponsor: Italian Ministry of University and Research; contract/grant number: FY 2004-2005 PRIN
Contract/grant sponsor: Portuguese Science Foundation FCT

Received 14 February 2007
Revised 3 December 2007
Accepted 4 December 2007

1. INTRODUCTION

The International Guadiana Bridge is a concrete cable-stayed bridge spanning the Guadiana River close to the seacoast in the southern Portugal, at the border with Spain (Figure 1). The bridge was designed by Câncio Martins and opened to traffic in 1991. Given the relatively severe wind and high seismic risk characteristics of the site, extensive studies were developed prior, during and after construction [1–3].

Despite the generally good performance under normal traffic and ambient conditions, the stay cables soon proved to be vulnerable to high-amplitude transversal vibrations, often not justified by simultaneous critical environment events. Moreover, since the cables are made of several parallel strands with individual protection sheathing, the absence of an effective locking system, like a jacket pipe, lays adjacent strands open to potential mechanical damage due to relative rubbing, which also produces a persistent and uncomfortable surrounding *rattling noise*.

In literature, different mechanisms that cause the raising of cable vibrations in cable-stayed systems are currently known. In particular, high-amplitude oscillations can arise in the stay cables, either due to direct rain–wind external excitation [4] or due to cable–deck boundary interactions related to internal resonance conditions between global (deck-dominant) and local (cable-dominant) modes [5]. The modal interactions can be classified either linear, if primary (1:1) resonance realizes direct excitation of the local mode, or nonlinear, whereas subharmonic (2:1) or superharmonic (1:2) resonance leads to *parametric excitation* [6–8] or *angle-variation excitation* of the local mode, respectively [9].

In particular, a purpose study on the Guadiana Bridge, developed at preliminary commissioning stage by Pinto da Costa *et al.* [10], specifically pointed out the vulnerability of certain cables to parametric excitation. Moreover, recent studies have demonstrated that the

Figure 1. The International Guadiana Bridge: (a) lateral view; (b) perspective view from Spain; (c) details of the deck–tower connection; and (d) details of the stay cables.

DOI: 10.1002/stc

highly dense bridge spectrum also realizes a variety of multiple internal resonances, which potentially enables other excitation mechanisms [11].

Starting from this literature background, this paper initially refers about the main features characterizing the current bridge dynamic behaviour, as given from both field visual inspections and periodic campaigns of vibration data collection during common traffic and wind service conditions (Section 3). The measured data are then used to update different finite element models of the bridge, which include a proper description of cable transverse motion [12, 13], with the aim of reaching a satisfying agreement between the experimental and numerical spectral properties (Section 4). Couples of interacting global and local modes are accurately selected, and the known sources of cable excitation are discussed as possible interpretations of the experimental evidence. On the light of an accurate comparison between the measurements and many numerical results, the cable–deck linear interaction realized by two internally resonant modes is recognized as critical excitation source for the cables exhibiting the highest amplitude oscillations (Section 5.1). On this respect, the bridge response to random deck excitation and moving loads is numerically evaluated to simulate different traffic conditions, and the results are compared with the experimental measurements (Section 5.2). Concluding remarks are finally drawn.

2. BRIDGE DESCRIPTION

The International Guadiana Bridge (Figure 1) is a cable-stayed bridge with a semi-fan cable arrangement, composed of a central span of 324 m, two lateral spans of 135 m and two transition spans of 36 m, with a resulting total length of 666 m (Figure 2). The deck structure is realized by a pre-stressed concrete box section, 18 m wide and 2.5 m deep, with internal concrete bracings at 4.5 m intervals. It is supported by two A-shaped concrete towers 100 m high, founded on piles on schist rock and also by 32 stay cable pairs anchored at each tower at equispaced 9.0 m intervals. The maximum length of the cables is of about 170 m for the central span and 150 m for the lateral spans. Each cable is a bundle made of a number varying between 22 and 55 monostrands, individually sheathed. The bundles have clamped collars at midlength (for the shortest cables) or at the third-lengths (for the other cables). Progressive numeration is used in the following to denote the cables suspended to each tower: from c1 to c16 from longest to shortest in the lateral span, and c17 to c32 from shortest to longest in the central span. When necessary, suffixes u(d) and p(s) are added to distinguish upstream (downstream) fan plane and Portugal (Spain) side.

3. VISUAL INSPECTION AND AMBIENT VIBRATION MEASUREMENT

3.1. Visual inspection

Careful site visual inspections of the bridge in-service behaviour allowed the recovering of useful information for a qualitative description of the most evident recurrent dynamic phenomena, and a comprehensive survey of the consequent time-evolving deterioration effects in different structural elements.

The most recent visual examination was conducted in March 2006 in optimal climatic conditions, with good weather and constantly moderate breeze coming from northwest, that is

DOI: 10.1002/stc

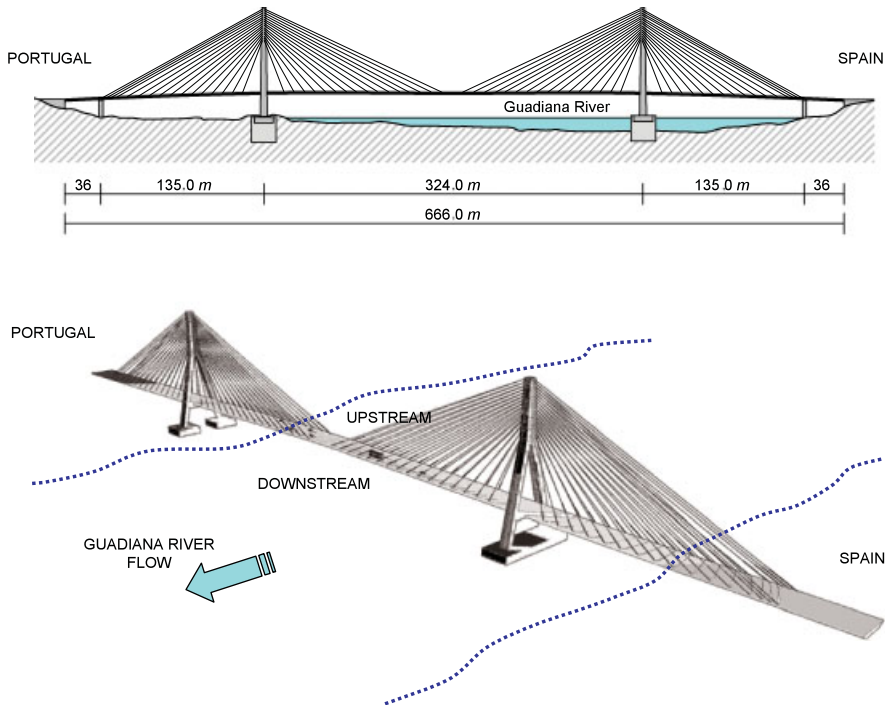

Figure 2. Sketch of the International Guadiana Bridge.

transversally incident to the bridge deck with lightly variable angle presumably ranged from 60 to 80°. A collection of frames captured during the inspection is presented in Figure 3. The bridge immediately showed persistent vibrations interesting most of the longest stays; in particular oscillations with moderately high-amplitude were localized in one or two stays for each fan. The maximum amplitude was visually noticed in the cable 29dp, which is the fourth cable starting from the deck midspan, towards Portugal, in the downstream fan, with reference to the River waterstream (Figure 3(a)). The same cable had been observed to experience high-amplitude vibrations also in previous inspections, namely during a test campaign in May 2003 [14], and in March 2004 [15].

Despite the complex nature of the cable spatial motion, the dominant vertical (*in-plane*) component of the transversal oscillations was clearly identifiable, with however no negligible component in the orthogonal (*out-of-plane*) direction. A rough evaluation of the cable 29dp vibration amplitude estimated the ratio with respect to different stays of the same fan in not less than 20 and 30 times. During the whole observation period, the persistence of the phenomenon throughout variable wind conditions (although almost stable) and irregular vehicular traffic was noticed. Temporary closure of the bridge carriageways also permitted to verify just a minor attenuation of the cable 29dp vibration level, which remained anyway higher with respect to the other stays.

Generally speaking, the overall inspection substantially revealed that although many cables suffer from more or less relevant vibrations under wind excitation, some cables exhibit higher levels of oscillation. These are specifically the four longest cables from the central span and an

DOI: 10.1002/stc

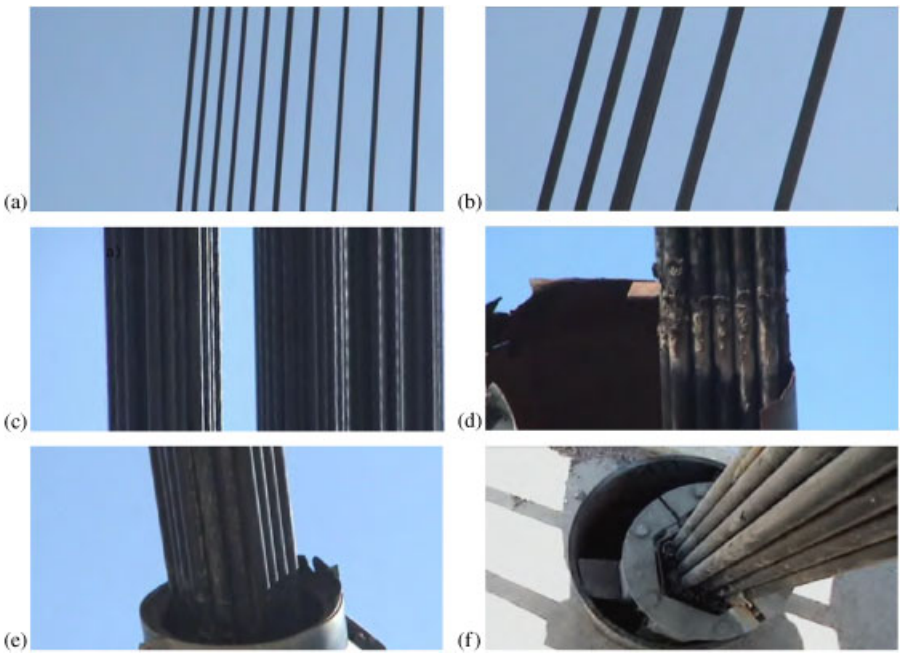

Figure 3. Frames from the visual inspection in March 2006: (a) instantaneous configuration of the vibrating cable 29dp; (b) cross-section *breathing*; (c) details of the rubbing strands composing the cables; (d) and (e) damage of non-structural components at the cable–deck connections; (f) accidental eccentricity of the cable passing through the cylindrical form tube.

ensemble of intermediate length cables from the lateral spans. Among these, episodes of very high vibration interest single cables, namely the third or the fourth longest cable of the central span.

The persistence of recurrent local oscillation events in these cables, even stronger than the observed ones, is indirectly confirmed by the detected failure of the clamped collars, used for locking the component strands. The consequent absence of cohesive links between adjacent strands allows single cables to behave as bundles of quasi-independent fibres, rubbing and beating against each other. Together with a disturbing *rattling noise*, the opposite-phase motion of the external strands produces a *breathing* effect of the cable cross-section, responsible for damage of non-structural components, like the protective ring seals and the damping neoprene sleeves at the cable–deck connections (Figure 3(b) and (c)). Moreover, the inspection of deviator guides at deck level showed damage for particular cables (Figure 3(d)–(f)).

3.2. Test campaigns

A first test campaign was developed in May 2003 with the purpose of generally characterizing the levels of vibration of cables and deck and for identifying the fundamental bridge frequencies and the installed cable force. During the three days of tests, generally good weather conditions were observed, with no rainfalls, temperature varying in the range 18–25°C, and with estimated

DOI: 10.1002/stc

variable average wind velocities lower than 12 m/s. Yet several episodes of large cable vibration were observed [14].

In order to characterize potential parametric excitation phenomena, simultaneous measurements were developed on the deck and on particular cables, at a height of about 2 m from deck, considering both vertical (deck)/in-plane transversal to the cable and lateral directions. A summary of the maximum vibration amplitudes recorded is presented in Table I.

A full identification of global modal parameters was performed based on the data collected during a second test campaign developed in March 2004 [15]. The test was based on the measurement of the ambient vibration response at a dense grid of points along the bridge deck and at two levels of each of the towers (Figure 4). Measurements were performed based on four independent triaxial seismographs that operated synchronously by means of GPS sensors after initial programming with a laptop. Two of those sensors were maintained fixed at a reference section located close to the third of the central span (position 17 in Figure 4), whereas the other two sensors roved all other upstream/downstream measurement points.

The complete test including records of 21-min duration in each of the 58 measurement points for the three directions was developed in two and a half days along which periodic

Table I. Summary of the recorded measures in the test campaigns.

Recorded motion	Acceleration (m/s^2)
Deck longitudinal component	0.012–0.048
Deck lateral component	0.025–0.069
Deck vertical component	0.101–0.389
Cable transversal component	0.4–10

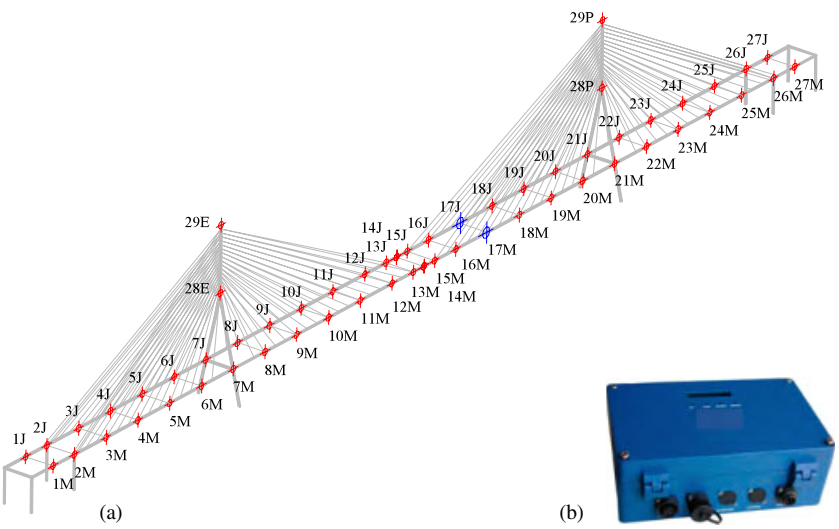

Figure 4. Experimental test campaigns: (a) complete set-up and (b) triaxial wireless recorder.

DOI: 10.1002/stc

measurements of the wind velocity were made. Despite the good weather condition, again with no rainfall, the average wind velocity varied in the range 2–14 m/s and different cable vibration conditions were observed, from almost no vibration, to significant vibration of almost all cables at the highest wind velocity.

3.3. *Identification of modal properties*

The processing of the ensemble of records based on different algorithms [16] allowed the identification of a total of 14 vibration modes in the range 0–3 Hz, with natural frequencies and general characteristics summarized in Table II, and with deck modal configurations represented in Figures 5 and 6. The filled circles in these figures mark the towers abscissae.

Individual cable frequency measurements allowed the identification of installed force using the vibrating chord theory. These data are relevant for the tuning of the finite element model described in Section 3. The obtained results are summarized in Figure 7, in which the vibrating cable 29dp is also marked.

Damping coefficients of global modes were also identified from the ambient vibration tests and are systematized in Table II. Although the degree of confidence in these estimates is lower than for frequency and mode shapes, an order of magnitude can be taken which is relevant for numerical simulations. Moreover, since continuous measurements were developed for the three days of test on the reference deck sections, it was possible to separate and process records associated with different average wind velocities. Figure 8 shows power spectral density function estimates in correspondence with some of those velocities, evidencing a widening of the peaks associated with bending frequencies with increased wind velocity, accompanied by the presence of numerous new peaks that reveal the influence of cable vibration. In particular, for the first vertical flexural mode V1 the average modal damping increases from 0.95 to 1.43 and 1.95%, for mean wind velocities of 2, 9 and 14 m/s, respectively. For the first lateral mode (L1), it increases from 1.84 to 2.28 and 2.43% and, for the first torsional mode (T1), from 0.37 to 0.51 and 0.47%.

Table II. Identified global modal properties of the International Guadiana Bridge.

	May 2004		
Mode number	f (Hz)	ξ (%)	Qualitative description of the modal shape
1	0.391	1.37	First vertical symmetric (V1)
2	0.537	2.23	First lateral symmetric (L1)
3	0.566	1.20	First vertical antisymmetric (V2)
4	0.845	—	Second vertical symmetric (V3)
5	0.952	0.69	Second vertical antisymmetric (V4)
6	1.035	0.51	Third vertical symmetric (V5)
7	1.299	0.54	Third vertical antisymmetric (V6)
8	1.445	0.47	First torsional (T1)
9	1.450	—	First lateral antisymmetric (L2)
10	1.660	0.63	Fourth vertical symmetric (V7)
11	1.812	0.65	Fourth vertical antisymmetric (V8)
12	1.880	—	Fifth vertical symmetric (V9)
12	2.251	0.59	Fifth vertical antisymmetric (V10)
14	2.578	0.46	Sixth vertical symmetric (V11)
15	2.783	1.48	Second torsional (T2)

DOI: 10.1002/stc

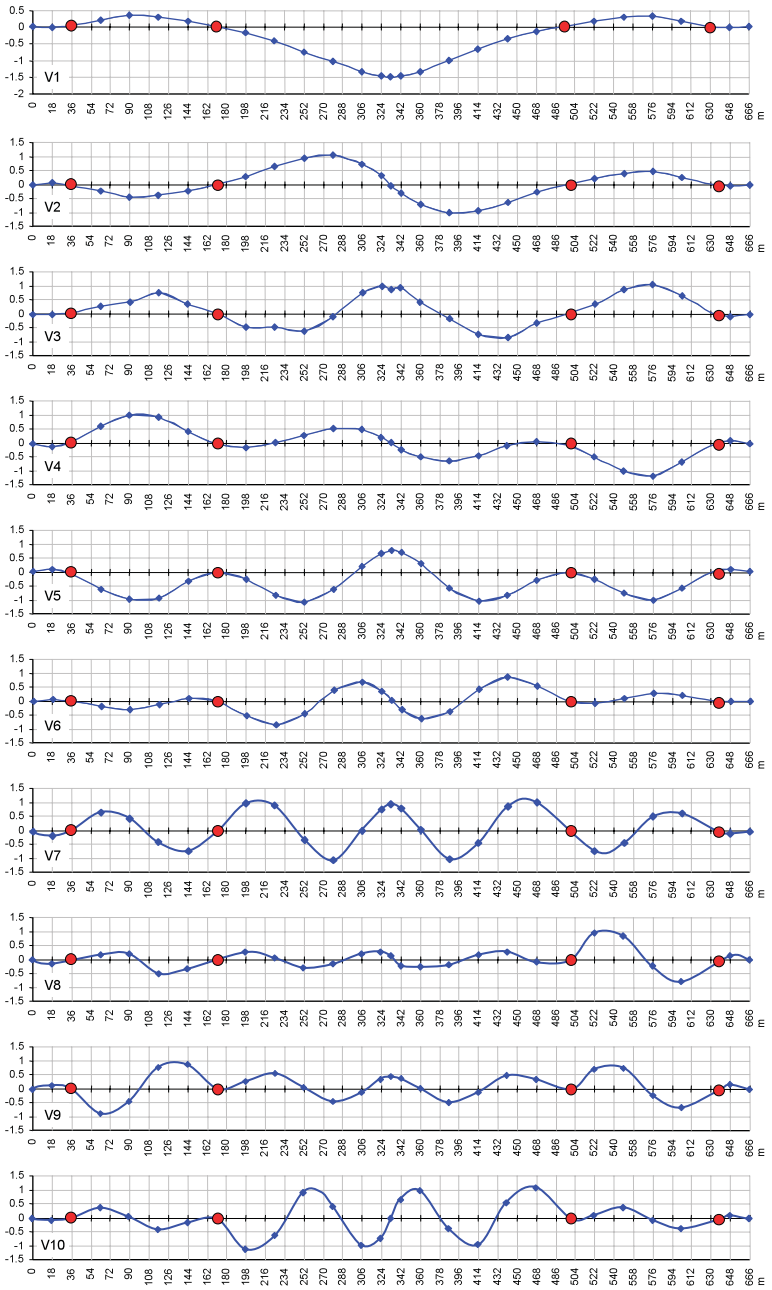

Figure 5. Identified vertical modal shapes.

This evident trend, which reveals an increasing aerodynamic contribution to modal damping, is numerically consistent with comparative measurements obtained in similar long-span cable-stayed bridges (see, for example, [17]).

DOI: 10.1002/stc

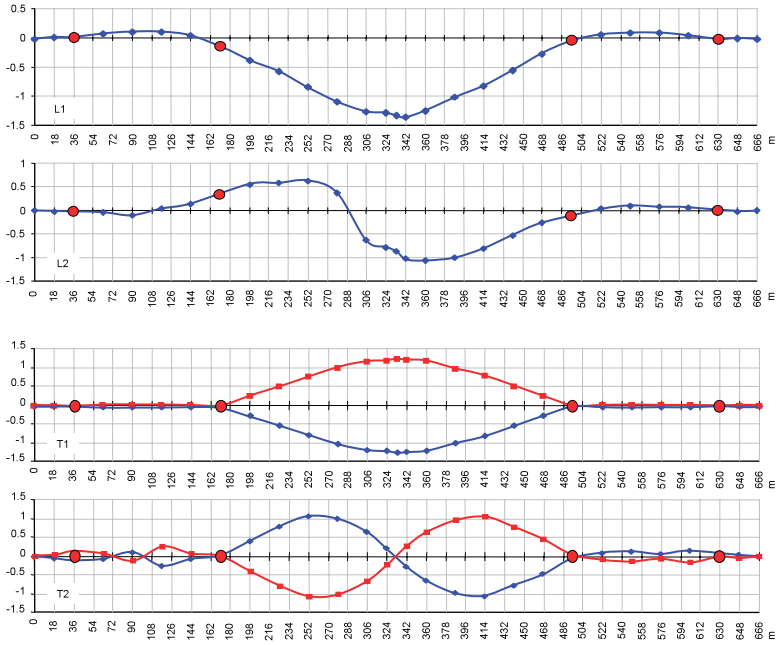

Figure 6. Identified lateral and torsional modal shapes.

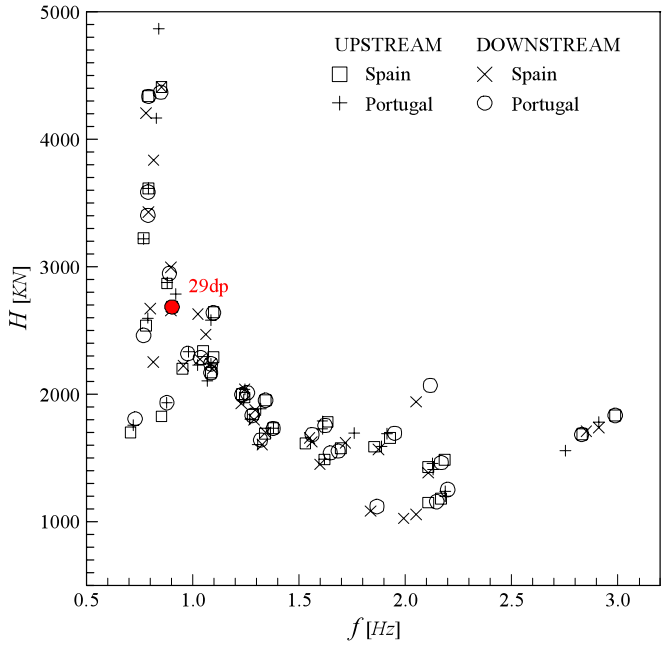

Figure 7. Identified cable frequencies versus calculated static tension.

DOI: 10.1002/stc

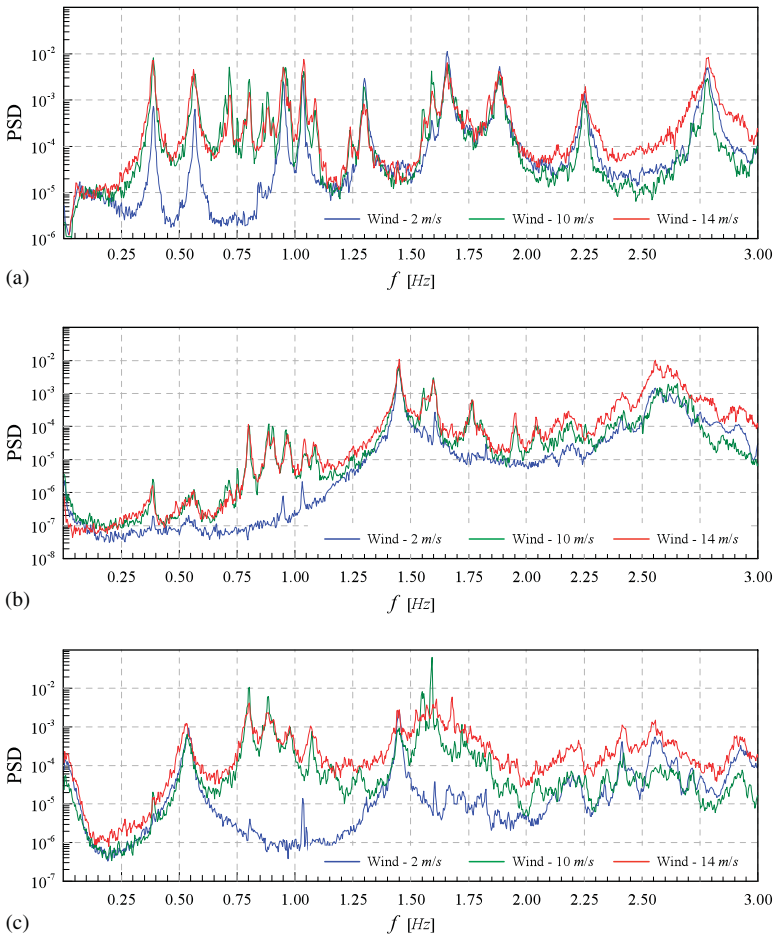

Figure 8. Power spectral densities functions at different wind velocities for: (a) vertical; (b) torsional; and (c) lateral motions.

3.4. Cable–deck interaction

The principal features of the bridge dynamic behaviour summarized in Table I allow a comparison between the first frequencies of deck modes and the frequency range of the fundamental local modes of the stay cables. It can be noticed that the range of fundamental mode frequencies of the cables covers several global frequencies, meaning that internal resonances may occur. Figure 9 shows the ratio r between the fundamental frequencies of each cable in the Portugal downstream fan and the deck frequencies of the lowest vertical global modes V1–V10 and the fundamental torsional mode T1. The first remark that could be immediately drawn is that ratios close to unity may enable 1:1 internal resonance conditions coupling the global modes V3–V10 and many of the longest cables (say c1–c14 in the lateral span, and c19–c32 in the central span).

DOI: 10.1002/stc

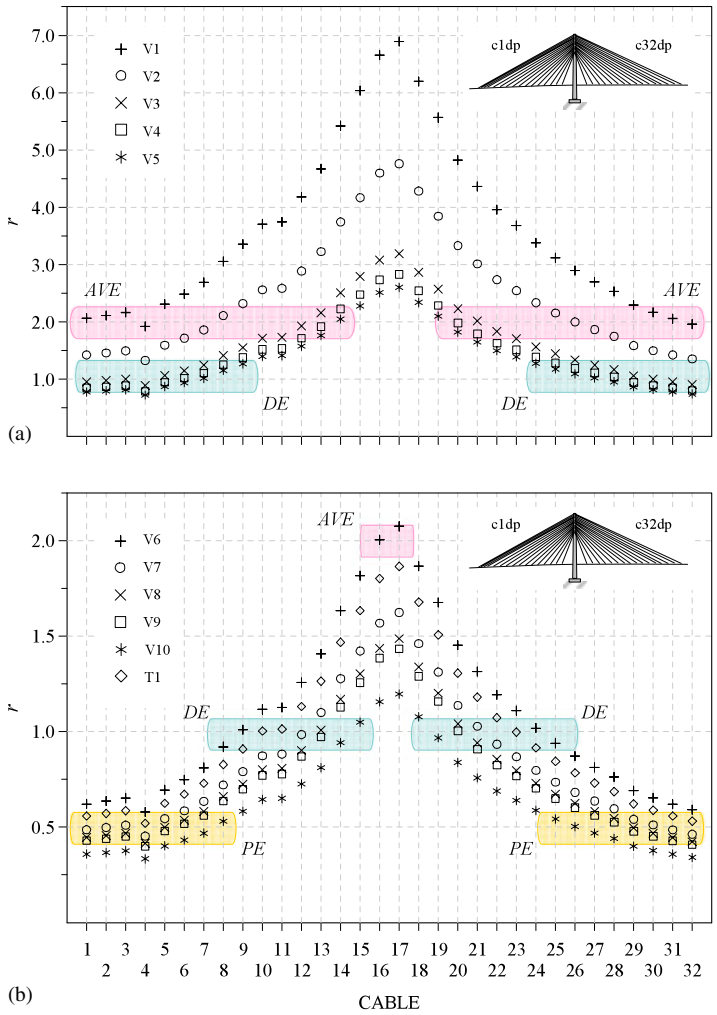

Figure 9. Ratio r between fundamental frequencies of the stay cables 1–32 and (a) frequencies of global modes V1–V5; (b) frequencies of global modes V6–V10, T1.

To systematically address the study of the cable–deck interaction mechanism, different critical regions are highlighted. First, the possible 1:1 internal resonance conditions (with small detuning $r \simeq 1$) define the region in which global modes may provide direct excitation (DE region) of the local modes. Second, subharmonic 2:1 ($r \simeq 0.5$) and superharmonic 1:2 ($r \simeq 2$) resonance conditions bound two nonlinear interaction regions, in which global modes may provide parametric (PE region) and angle variation excitation (AVE region) of the local modes, respectively. It can be immediately recognized that, while the only longest cables (c1–c8, c25–c32) should be considered really vulnerable to parametric excitation due to the higher modes (V6–V10, T1), all the bridge stay cables are indeed exposed to both direct excitation and angle variation excitation. In particular, many long cables of the lateral (c1–c8) and central span

DOI: 10.1002/stc

(c24–c32) may suffer direct excitation from three global modes (V3, V4 and V5), whereas the only longest cables of the lateral (c1–c4) and central span (c30–c32) lay open to angle variation excitation from the global mode V1.

Recalling that nonlinear interaction mechanisms generally require high amplitudes in the oscillating global mode to realize a significant energy transfer to the local mode [7, 9], the recorded deck acceleration amplitudes also represent a crucial analysis issue to be discussed.

Looking at the measure data collected in Table I, the deck accelerations are generally very low, the vertical component amplitude being one order higher than the longitudinal component, and around five times the lateral one. Differently and despite considerable scatter, the measures of the cable accelerations at about 2.5 m from the deck anchorage may reach around one hundred times the vertical deck acceleration, which corresponds to maximum amplitudes of around 0.50 m at cable midspan, considering monofrequent oscillations on the first mode. This value approximatively corresponds to 2.6 times the cable diameter and substantially fits the visual estimates of 1.0 m peak-to-peak oscillation.

It should be noticed that these oscillations occurred for moderate average wind velocities no greater than 14 m/s. Looking at the frequent occurrence of cable vibration during tests, a variety of critical situations were clearly correlated with particular combination of wind velocity and direction, each involving different stay cables and presenting different features. Generally, moderate oscillations systematically occur for moderate wind velocities, in the range 10–15 m/s, involving a significant number of cables. Particularly interesting observations regard the sudden appearance of high-amplitude oscillations localized in just one or a small group of stay cables (normally, among the largest of the central fan or the mid-length cables of lateral fan). These oscillations were observed to persist even for various hours without vanishing neither for falling

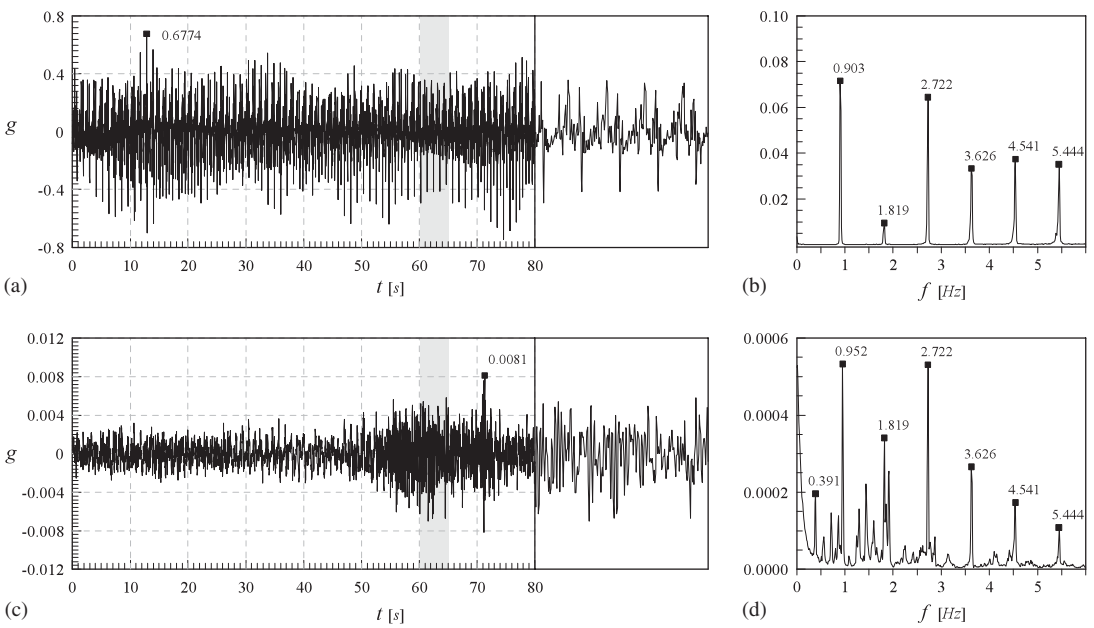

Figure 10. Measured time histories and power spectra at cable c29dp: (a) and (b) cable span (2.7 m from the deck); (c) and (d) anchorage level.

DOI: 10.1002/stc

down of the wind velocity, whereas the oscillation amplitude varied for slight modification of the wind direction.

Among several acquisitions, the significant records shown in Figure 10 have been extracted to be discussed. They represent simultaneous acceleration time histories measured on the cable c29dp deviator guides (Figure 10(a)) and at the cable–deck anchorage (Figure 10(c)), for a total acquisition time of 81.9 s. It is worth noting that the cable experiences high-amplitude oscillation in the whole recording period, with peak accelerations around $0.68g$ at time 12.8 s, or even $0.74g$ at time 74.56 s. Differently, the deck exhibits much lower amplitude acceleration, with maximum value $0.0082g$ at time 71.16 s, whose ratio with respect to the cable peak is about $\frac{1}{90}$.

Figures 10(b) and (d) show the power spectral content of the two records. The first in-plane cable mode corresponds to a frequency peak around 0.903 Hz, whereas higher equispaced sharp peaks characterize the higher frequencies (Figure 10(b)). Differently, the deck has a dense frequency content, with several close peaks. Many of these peaks coincide with the cable frequencies, confirming that significant local oscillations can someway influence at least the low-amplitude deck response. The remaining peaks can be reasonably associated with the global modes. In particular, an important peak can be identified at a frequency of 0.952 Hz, which is close to the fundamental cable frequency. The consequent 1:1 internal resonance condition between a global and local mode could be therefore potentially responsible for the direct cable excitation, through the support motion produced by the deck oscillations at the anchorage.

4. FINITE ELEMENT MODEL

A three-dimensional finite element (FE) model of the Guadiana Bridge has been developed for comparison with the measured results (Figure 11). The model describes the bridge response

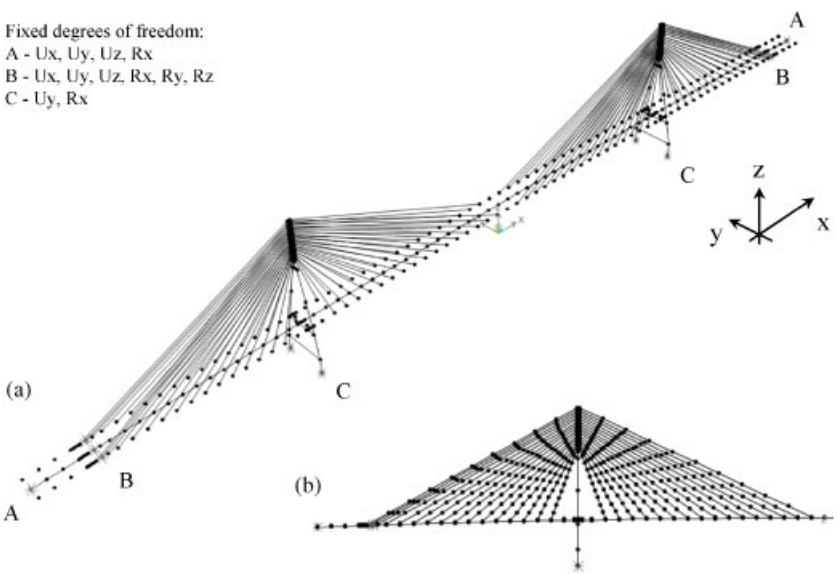

Figure 11. FE models of the Guadiana Bridge: (a) OECS model and (b) modelling of the cable stays in the MECS model.

DOI: 10.1002/stc

according to the modelling proposal by Wilson and Gravelle [18] for the dynamic analysis of cable-stayed bridges. In particular, the vertical, transversal, axial and torsional stiffness properties of the deck box cross-section are concentrated in a single central longitudinal spine, made of 92 two-node beam elements, which follows the curvilinear deck profile. Additionally, 64 couples of transversal offset rigid links connect the spine nodes with each of the 128 downstream and upstream cable anchorage points. The whole translational inertial properties of the deck are instead divided in two equal lumped mass hosted by the cable anchorage points, so that the spine possesses just the longitudinal rotational inertia needed to correct the eccentricity of the section shear centre from the geometric centroid. Beam elements with variable cross-section represent the towers.

The geometric and mass properties of each structural element have been initially desumed from the available information about the bridge design project [1, 3, 19]. With respect to the material characteristics, concrete grades in the deck, pylon and piers ranged from 30–45 MPa, and the corresponding elastic modulus used in the FE model were 42–46 GPa. The cable steel elastic modulus is 195 GPa.

Since this study is not strictly focused on the soil–structure interaction, towers are assumed fixed at the foundation level. The other fixed degrees of freedom are reported in Figure 11. The spine is connected to the support strut of the towers by rigid links simulating the behaviour of the bearings, which are assumed to substantially avoid relative vertical and transversal displacement, but to enable small relative rotations.

For the purpose of this study, careful attention has been devoted to the modelling of the stay cables. Several solutions have been proposed in the literature to overcome the limits of the single truss model (*one-element cable system* – OECS), originally proposed by Ernst [20], and also adopted in the scheme by Wilson and Gravelle [18]. This approach, which reproduces just the bridge deck motion, does not anyway account for the local cable transversal motion, and thus misses to describe its interaction with the global dynamics. Among other alternatives, a linearized description of the cable transversal motion has been successfully employed [12, 21]. Following this approach, each stay cable is modelled through a straight linkage of pre-tensioned truss elements (*multi-element cable system* – MECS). A preliminary evaluation of the geometric stiffness ensured by the elements pre-tension is required to avoid transversal instability. The transversal cable motion is then fully captured by the displacement of the additional nodes introduced along the cable length.

Two FE models of the Guadiana Bridge are discussed in the following. Initially, an OECS model (Figure 11(a)) is assembled for preliminary analyses on the bridge static response to dead loads and for first comparison of the global modes with the identified ones. Subsequently, a refined MECS model (Figure 11(b)) is obtained meshing each cable with 10 truss elements. This number of elements has been proved to ensure frequency convergence, without simultaneously overcoming reasonable computational effort [13]. Compact circular cross-section is assigned to each cable, with the effective area of the strands bundle. Lumped masses at the internal nodes wholly account for the cables inertial properties.

4.1. Modal analysis and model updating

Nonlinear static analyses have been firstly performed on the OECS model to evaluate the modified bridge geometric configuration undergoing large displacement under self-weight load, using a tangent stiffness iterative-incremental procedure. The maximum displacement obtained

DOI: 10.1002/stc

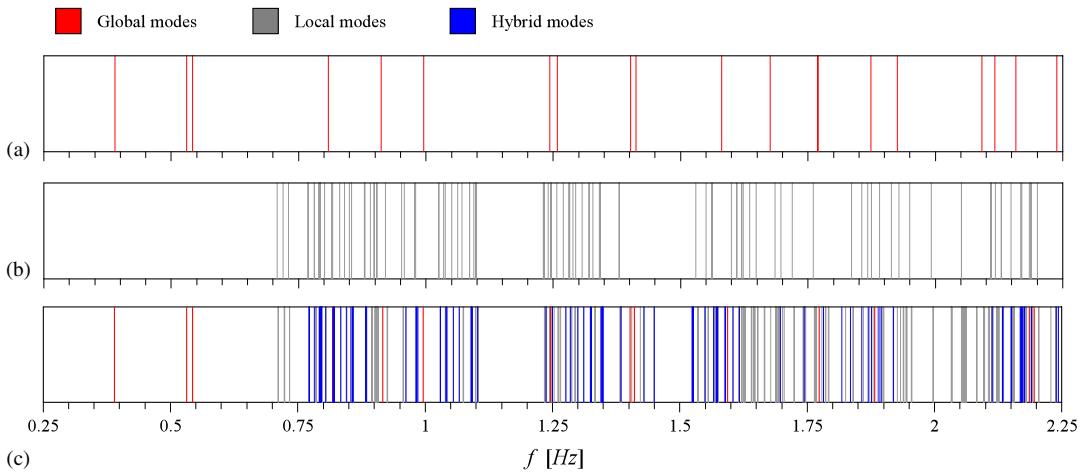

Figure 12. Spectrum content of the Guadiana Bridge: (a) OECS model frequencies; (b) experimental cable frequencies; and (c) MECS model frequencies.

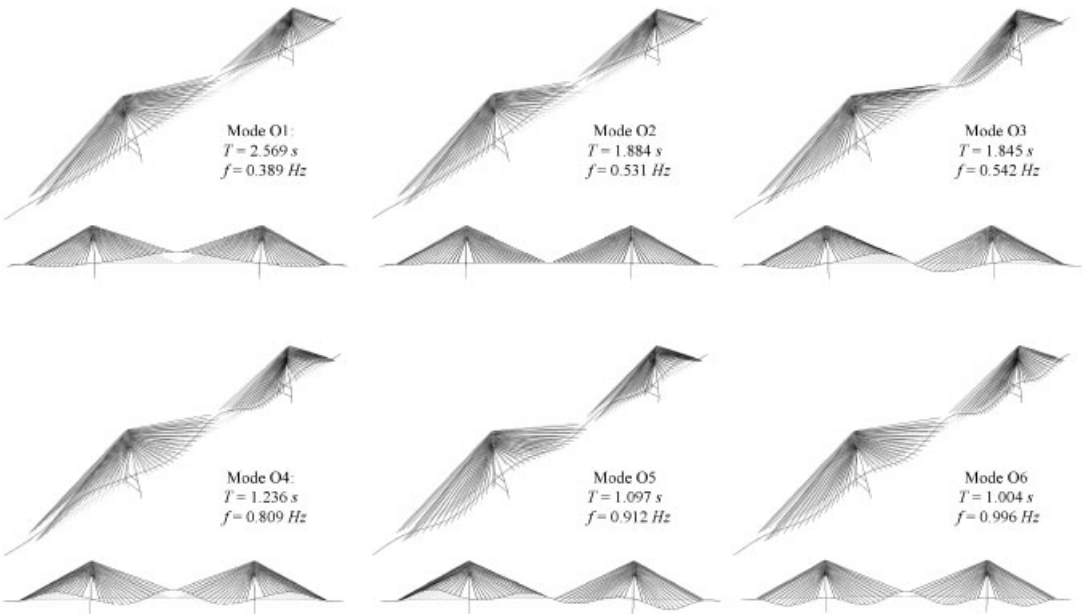

Figure 13. OECS model of the Guadiana Bridge: selection of global modes.

DOI: 10.1002/stc

Table III. Comparison between the identified and the numerical FE frequencies.

Experimental		OECS FE model			MECS FE model			MECSu FE model		
Mode	f (Hz)	Mode	f (Hz)	Δf (Hz)	Mode	f (Hz)	Δf (Hz)	Mode	f (Hz)	Δf (Hz)
V1	0.391	O1	0.390	−0.001	M1	0.390	−0.001	M1	0.396	+0.005
L1	0.537	O2	0.530	−0.007	M2	0.531	−0.006	M2	0.537	0.000
V2	0.566	O3	0.542	−0.024	M3	0.543	−0.023	M3	0.563	−0.003
V3	0.845	O4	0.809	−0.036	M38	0.819	−0.026	M44	0.852	+0.007
V4	0.952	O5	0.912	−0.040	M73	0.916	−0.036	M75	0.951	−0.001
V5	1.035	O6	0.996	−0.039	M84	1.004	−0.021	M88	1.038	+0.003
V6	1.299	O7	1.244	−0.054	M127	1.246	−0.053	M149	1.324	+0.025
T1	1.445	O10	1.444	−0.001	M169	1.402	−0.043	M174	1.449	+0.004
L2	1.450	O8	1.256	−0.194	M171	1.411	−0.039	M177	1.452	+0.002
V7	1.660	O11	1.579	−0.081	M213	1.593	−0.067	M251	1.712	+0.052
V8	1.812	O13	1.764	−0.048	M265	1.774	−0.038	M290	1.915	+0.103
V9	1.880	O14	1.874	−0.006	M285	1.883	+0.003	M308	2.047	+0.167
V10	2.251	O19	2.232	−0.019	M383	2.251	+0.000	M421	2.454	+0.203

in the bridge midspan section is around 1.48 m, which approximately corresponds to $\frac{1}{220}$ of the central span length and is close to that of similar cable-stayed bridges (see, for example, the prototype bridge in [22]).

The final tangent stiffness matrix has then been used to start the linear modal analysis. It has been finally noted that just negligible changes with respect to the unloaded bridge frequencies affect the lowest global modes. Parametric investigations, here not reported for the sake of brevity, have shown that minor increments of the first frequency (namely less than 4%, and even minor for the higher frequencies) are reached only for improbable multipliers of the self-weight (surely greater than 2.1). Thus, the frequencies and modes of the unloaded bridge are considered a faithful reference in the following.

The spectrum of the OECS model is reported in Figure 12(a) in the frequency range 0.5–3.0 Hz, whereas a selection of modes is reported in Figure 13. They essentially involve the spine deflection in the vertical (see, for example, the modal shapes of modes O1, O3) and the horizontal plane (O2) or the spine torsion along its longitudinal axis. From the comparison with the identified frequencies (see Table III), it can be observed that the OECS model closely describes the experimental spectrum, since the maximum frequency difference, related to the identified vertical mode V7, is anyway less than 0.1 Hz. Qualitatively, it can be observed that the modes of the OECS model are generally more flexible (smaller frequencies) than the identified ones, with increasing frequency differences for the higher modes, at least up to V7. A flipping between the first torsional mode (O10) and the second lateral one (O8) with respect to the identified sequence could also be noted.

The information furnished by the test campaigns is then employed to enhance the reliability of the MECS model in describing the real bridge dynamics. On this respect, avoiding any preliminary static analysis, the actual tensile forces in the cables have been updated from the initial design values (pre-tensions) to those calculated from the identified cable frequencies. These frequencies are reported in the spectrum of Figure 12(b). In particular, this updating should allow the MECS model to reproduce better the experimentally assessed resonance conditions between local and global modes, which is a crucial issue for an effective investigation on the cable–deck interactions.

DOI: 10.1002/stc

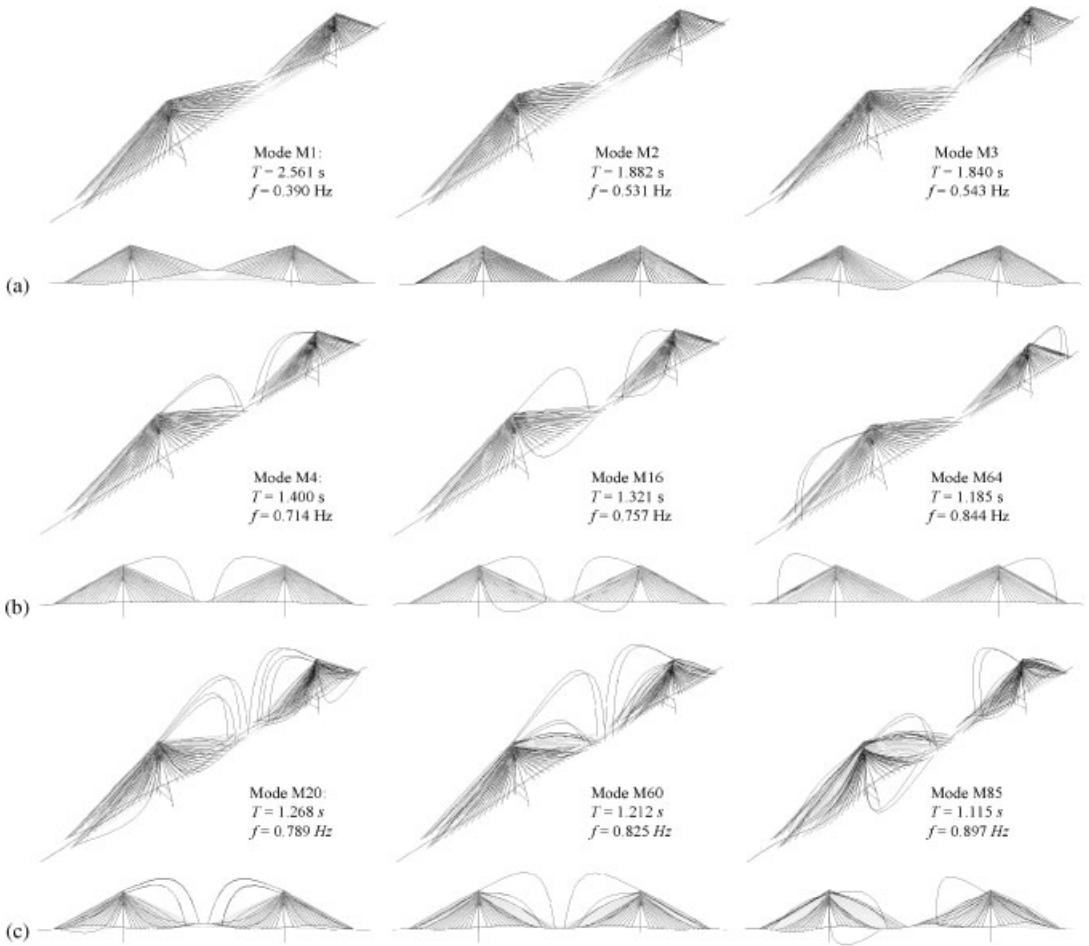

Figure 14. MECS model of the Guadiana Bridge: selection of (a) global modes; (b) local modes; and (c) hybrid modes.

In the considered frequency range (0.5–3.0 Hz), the MECS model presents a dense spectrum (Figure 12(c)), formed by several close frequencies related to global, local and *hybrid* modes (denoted by M1, M2, etc. in the following). The global modes closely replicate those previously obtained with the OECS model, whereas small difference could be noticed in the frequencies. The introduced MECS description of cables has a light stiffening effect on all the global modes (Table III), whose frequencies are systematically increased, and then also closer to the identified one. As the main consequence, the flipping between the torsional and the lateral mode, which is less sensitive to this effect, disappears. A selection of the lowest global modes is reported in Figure 14(a).

In the same frequency range, a large number of local modes, which essentially involve the transversal three-dimensional cable motion, with almost negligible participation of the main structure (deck and towers), have been also obtained. A selection of these modes is reported in Figure 14(b). They describe only the local cable dynamics, which in the performed linear modal

DOI: 10.1002/stc

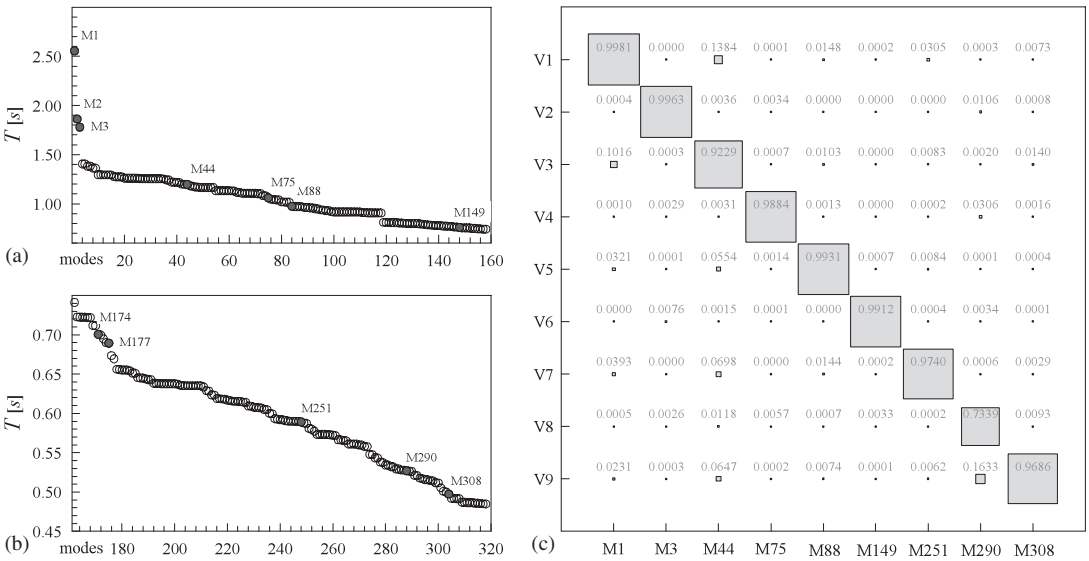

Figure 15. The MECS model of the Guadiana Bridge: (a) and (b) mode periods; (c) modal accordance criterion.

analysis is really quasi-independent of the deck motion, until no internal 1:1 resonance conditions between global and local frequencies exist. Once this condition is verified, a strong linear interaction between the two frequencies arises, and the involved modes undergo a combination process leading to some hybrid modal shapes, in which cables and deck equally participate. A selection of hybrid modes is reported in Figure 14(c).

The mode hybridization has been recently proved to follow from a veering phenomenon between the resonant frequencies [13] and can be really recurrent in complex structures like the Guadiana Bridge, with a dense frequency spectrum and a large number of cables. However, the adopted MECS-type modelling of the stay cables has been also verified to correctly describe the realized modal interaction.

Taking the experimentally identified modes as reference, a preliminary qualitative comparison confirms that the selected global modes of the MECS model closely match the identified modal shapes. Furthermore, a numerical evaluation of the difference between the model and the bridge frequencies is reported in Table III. It can be observed that the FE modes are typically more flexible than the corresponding identified ones, since they systematically present smaller frequencies, with the vertical flexural mode V9 being the only exception. However, the maximum obtained difference is around 0.067 Hz (mode V7), corresponding to a percentage difference less than 5%, so that only minor adjustments of the FE model have been deemed necessary.

An updated FE model of the bridge (denoted by MECSu in the following) has been formulated by introducing small corrections of the design mechanical properties. In particular, the variation in a few selected mechanical parameters (Young modulus and vertical inertia moment) has been tuned letting the model spectrum address the target identified frequencies as much as possible (see Table III). Moreover, the rigid links connecting the deck to the tower strut have been replaced by purposely defined spring elements in order to simulate an axially rigid but transversally elastic shear behaviour of the bearings. A significant improvement of the model

DOI: 10.1002/stc

has been achieved especially for the lower modes, since the mean quadratic frequency difference for the first 10 modes is reduced by more than 70%.

As a further measure of the match between the MECSu model and the experimental measures, the *modal assurance criterion* (MAC) has also been applied to the vertical global modes, up to the fifth symmetric one (V9). As can be observed from Figure 15, excellent agreement is verified. In fact, MAC values close to unity (and always greater than 0.96) are obtained self-correlating each other the corresponding FE and the identified modes, whereas MAC values close to zero (and always less than 0.04) are obtained cross-correlating the non-corresponding modes, with only a few exceptions.

5. LOCAL VIBRATION ANALYSIS

5.1. Internal resonance conditions

The modal shapes of the MECSu model generally show a significant level of coupling between the deck and cables motion. In particular, it is known that the presence of numerous local and hybrid modes may significantly affect the bridge response to dynamic loads in the nonlinear and even in the linear analysis field [21].

To measure the mode localization level of the ith mode in the jth cable, a normalized localization factor $\Lambda_{i,j}$ has been recently proposed [13]. It was defined to immediately distinguish between pure local cable ($\Lambda_{i,j}$ close to unity) and deck global modes ($\Lambda_{i,j}$ close to zero) and to recognize also different hybridization levels (all intermediate values)

$$\Lambda_{i,j} = \frac{(\mathbf{R}_j\boldsymbol{\phi}_i)^{\mathrm{T}}\mathbf{M}(\mathbf{R}_j\boldsymbol{\phi}_i)}{\boldsymbol{\phi}_i^{\mathrm{T}}\mathbf{M}\boldsymbol{\phi}_i}, \quad \Lambda_{i,j} \in [0, 1] \tag{1}$$

where $\boldsymbol{\phi}_i$ is the ith mode, $\mathbf{M}$ is the mass matrix of the MECS-type model and $\mathbf{R}_j$ is a diagonal matrix of ones and zeroes that allows a selection of the degrees of freedom along the jth cable length.

Physically, the localization factor represents the ratio between the kinematic energy stored in the cable domain and the total kinematic energy of the system undergoing monofrequent (f_i) free linear oscillations. Practically, making reference to this factor, originally defined for continuous models, may greatly benefit from the finite element discretization, since many computer programs for vibration analyses employ solution procedures for the modal problem which include normalizing the mode amplitudes to satisfy the condition $\boldsymbol{\phi}_i^{\mathrm{T}}\mathbf{M}\boldsymbol{\phi}_i = 1$. Thus, the assessment of the mode localization degree from Equation (1) reduces to the evaluation of the factor numerator, with obvious computational advantages.

Since the present analysis of the FE model is focused on isolating possible sources of local oscillation which could regard the vibrating cable 29dp, major attention is devoted to the internal resonance conditions associating its local frequency with that of global or hybrid modes. These modes, if externally excited, could potentially transfer part of the mechanical energy to the cable.

In particular, a pure local mode of cable 29dp is the M72 of the MECSu model, with frequency $f_{72} = 0.908$ Hz and a localization factor $\Lambda_{72,29\mathrm{dp}} = 0.941$, depicted in Figure 16. As for many global modes, its frequency is really close to that identified during the test campaigns. Thus, recalling also Figure 9, potential occurrence of nonlinear excitation mechanism, like

DOI: 10.1002/stc

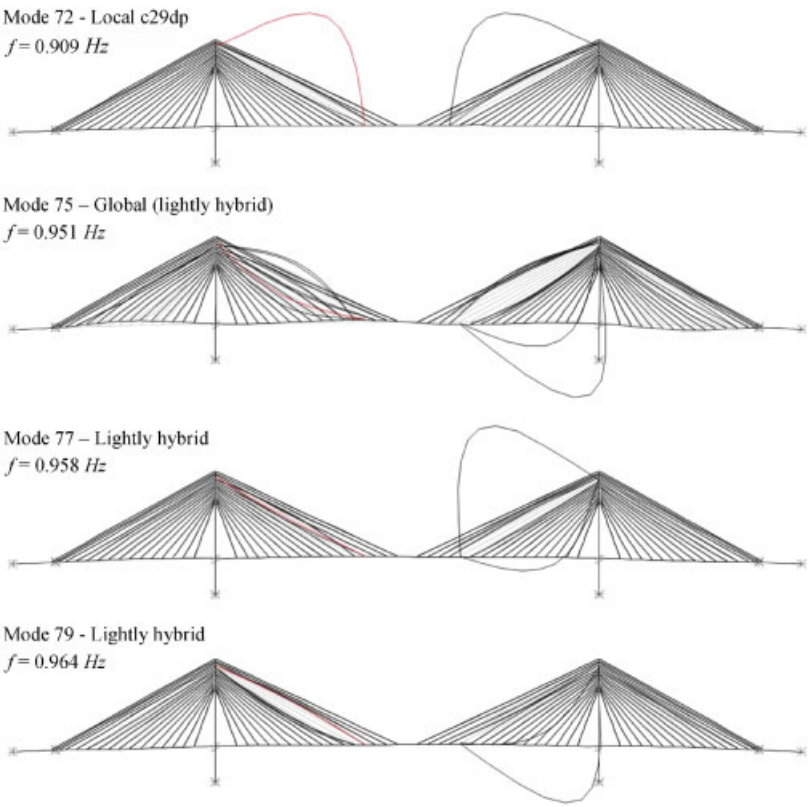

Figure 16. Resonant modes of the MECSu model.

parametric excitation from vertical modes V8, V9 (M288, M301 in the MECSu model) or angle variation excitation from mode V1 (M1), and also linear excitation from mode V4 (M75) can be suspected.

The effective relevance of different nonlinear phenomena in the dynamics of the Guadiana bridge has been already studied with regard to the parametric [14, 24] and to the angle variation excitation mechanism [11]. In the first case, simultaneous measurements of deck and cable have been obtained during events of large cable oscillation and possible parametric effects have been investigated, namely the 2:1 resonance. It has been, however, concluded that the threshold amplitude of deck acceleration for parametric excitation would be much higher than the one measured. In the second case, a refined analytical model of a simple cable-stayed beam was developed, which is able to synthetically reproduce the bridge spectrum of resonant frequencies, taking also into account the system geometric nonlinearities. Despite the absence of an amplitude threshold for the raising of the coupled nonlinear oscillations between the global mode at lower frequency and the local mode at higher frequency, the analysis findings revealed that the measured deck acceleration level (recall Table I and Figure 10) was unable to justify the amplification observed in the cable 29dp oscillation. However, it should be noted that the nonlinear modal coupling was investigated by means of a reduced model including at most three resonant modes (1:2:2), whereas the FE model reveals a highly dense

DOI: 10.1002/stc

spectrum with many similar modes with different levels of hybridization, interacting at the selected frequencies.

Excluding nonlinear excitation mechanisms, focus is made here on the primary resonance condition between the local mode M72 and the global mode M75, which is depicted in Figure 16. It corresponds to the identified second symmetric vertical mode V4, and its frequency $f_{75} = 0.951$ Hz realizes a ratio $r = 0.961$ with the local mode M72. Moreover, its modal shape presents light hybridization ($\Lambda_{75} = 0.164$), involving the same cable 29dp and other cables, especially c28dp. The closeness of other hybrid modes (M77 and M79, see Figure 16), unless with lower hybridization factors, evidences that the modal properties are already strongly affected by this cable–deck linear interaction.

In the following linear analyses, it is considered that similar frequency ratios are also realized among the longest cables and the identified global modes V3–V5. In order to isolate the effects of the global–local resonance, different dynamic actions are applied on the bridge deck. Since the local modes negligibly participate to deck loads, while no external actions are transversally applied along the cables, the anchorage vertical motion is the only excitation source for cable oscillations.

5.2. *Vibration characteristics of the forced response*

5.2.1. Random deck excitation. To investigate the internal resonance effects on the bridge motion, random excitation is initially applied to the deck. A vertical point load is applied to the spine of the FE model at the anchorage section of cable c29dp (section Decka29p). A white noise has been employed to define a 1000 s long amplitude history, with constant time step of 0.04 s. The signal was suitably filtered to retain the frequency spectrum band 0.7–1.3 Hz, which includes the global modes V3–V5 (M44, M75 and M88 of the MECS model), together with the local modes of longest cables c27–c32 in the bridge midspan. The maximum amplitude after filtering is about 6.351 N at time 395.82 s.

The bridge response to white noise has been calculated integrating the modal linear equations of motion, considering all the lowest bridge modes with frequency less that 1.5 Hz. Since modal damping should be introduced, the identified values reported in Table II have been used for the global modes, whereas constant percentage damping of 0.1% has been assigned to all the remaining local modes, according to experimental results, which furnish values ranging from 0.08 to 0.12%.

Figure 17 presents the obtained time histories related to the vertical displacement of the bridge deck (Figure 17(a)), and the midspan transversal displacement of the cables c27dp–c32dp (Figures 17(b)–(g)). The maximum and minimum displacement amplitudes are suitably marked. The frequency content of each time history is instead reported in Figures 17(h)–(n), in which the fast Fourier transform (FFT) amplitudes are depicted, and the frequency of the highest peak is marked.

Looking firstly at the deck response, a narrow frequency peak corresponding to the global mode M44 can be recognized (Figure 17(h)), together with three close peaks, which should be related to the hybrid modes M75, M77 and M79, and are partially overlapped in the frequency range 0.950–0.955 Hz. The maximum displacement and the peak FFT amplitude are also reported in Table IV.

Focusing on the cable response, it could be initially noticed that the frequency content of each displacement history is mainly characterized by the dominant peak of the corresponding local mode. However it is worth noting that, even if the longest cables c30dp, c31dp and c32dp are

DOI: 10.1002/stc

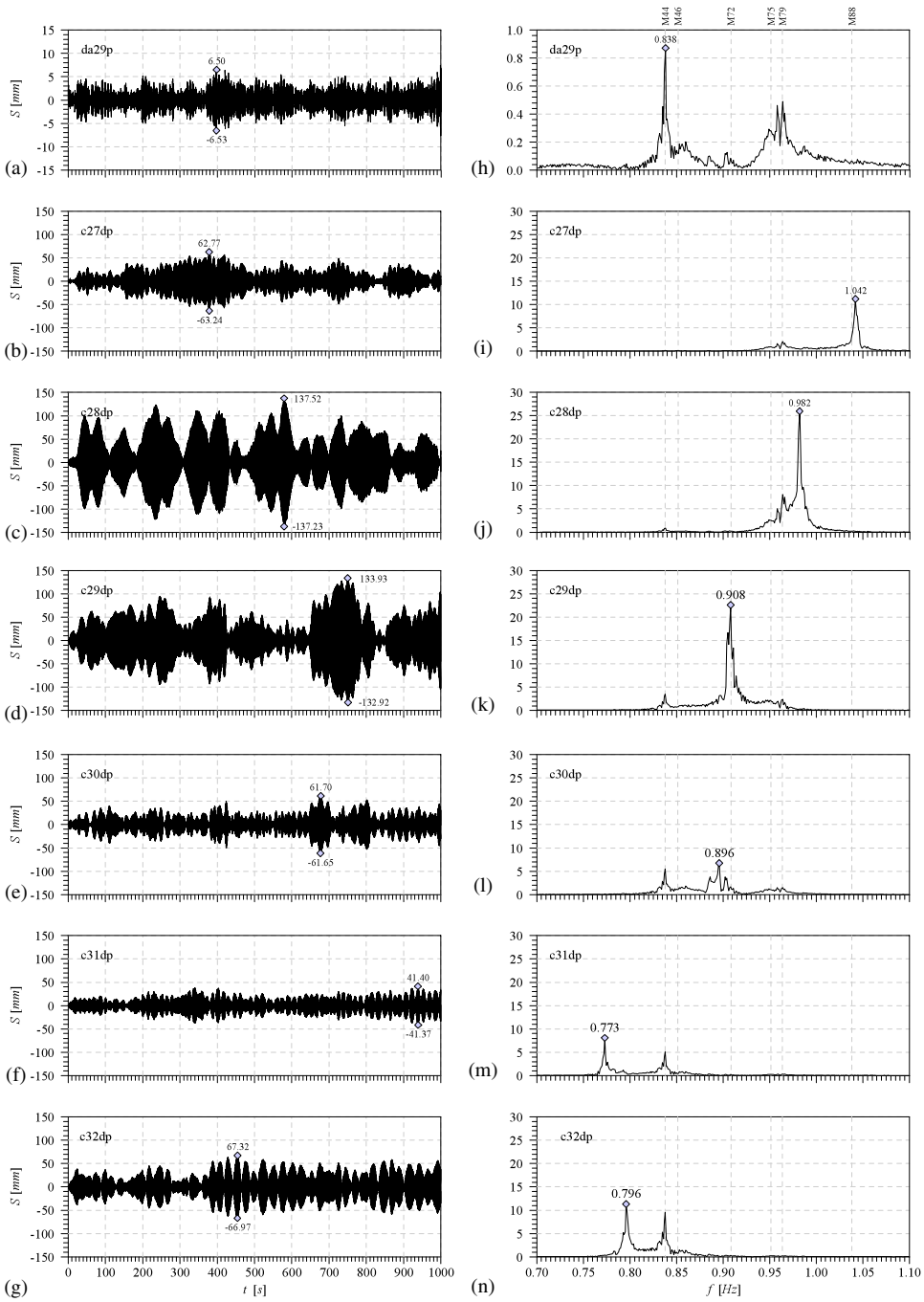

Figure 17. Bridge response to random excitation: (a)–(g) displacement time histories and (h)–(n) amplitudes of the FFT.

DOI: 10.1002/stc

Table IV. Peak displacement of the bridge response to random excitation.

	S_{max} (cm)	s_{max}	A_{max} (cm)	$f(A_{max})$ (Hz)
Deck da29p	6.5	—	0.87	0.838
Cable c27dp	62.8	9.7	11.21	1.042
Cable c28dp	137.5	21.2	25.94	0.982
Cable c29dp	133.9	20.6	22.62	0.908
Cable c30dp	61.7	9.5	6.75	0.896
Cable c31dp	41.4	6.4	8.09	0.773
Cable c32dp	67.3	10.4	11.33	0.796

more flexible, the cables c28dp and c29dp exhibit highest peaks. This relevant result is qualitatively consistent with both the visual inspection and the *in situ* measurements. It is really due to the 1:1 internal resonance with the externally excited group of global modes M75, M77 and M79, whose frequencies are also present in the cable displacement histories (Figures 17(j) and (k)). Between the two cables, the c28dp peak is lightly higher, probably due to the minor internal detuning with the hybrid modes. Looking at the time histories (Figures 17(c) and (d)), the interaction between close resonant modes is also revealed by a beating-type behaviour. The maximum displacements S_{max} are significantly higher than those of other cables, and up to 20 times that of the deck (see the ratio s_{max} in Table IV). Nonetheless, these results still partially justify the measured cable vibration amplitude (see, in particular, [15]).

Finally, it could be noted that internal resonance subsists also between the global mode M44 and the local mode of cable c32dp, and so in many other cases. Even if from Figures 17(g)–(n) qualitatively similar remarks could be drawn (again evidencing for example close frequency peaks in the FFT amplitude, and beating displacement amplitude), the relevance of the interaction phenomenon is not amplified due to a minor modal coupling, whereas a stronger hybridization of the modal shapes is required to enable the transfer of mechanical energy to the cable in the linear field.

5.2.2. Moving load. A vehicle-type load made of three non-eccentric vertical forces moving along the deck longitudinal spine has been selected as second possible excitation source for bridge FE model. Each force has a realistic amplitude of 40 kN, so that the whole force train approximately reproduces the quasi-static effects of a road track. Since the analyses were not focused on the vehicle–bridge interaction, no additional refinements were introduced to model the non-periodic nature of the traffic load, neither the stiffness and inertial properties of the vehicle nor the contact effects due to the pavement roughness.

A cyclic loading history made of three consecutive passages of the force train with constant velocity has been defined. The bridge response has been calculated directly integrating the model equations of motion with constant time step of 0.02 s. Parametric analyses have been performed varying the load velocity in the range 60–110 km/h. To achieve the goal of the study, the displacement time histories of a few nodes of interest have been extracted, regarding the interacting global and local modes.

Figure 18 is referred to the case of load velocity 85 km/h, which corresponds to a total integration period of 84.6 s, comprehensive of three consecutive passages of the force train, with a tail of free oscillations. The vertical displacement history of the deck at the cable c29dp anchorage (node A, Figure 18(a)) is compared with the transversal in-plane response of the cable

DOI: 10.1002/stc

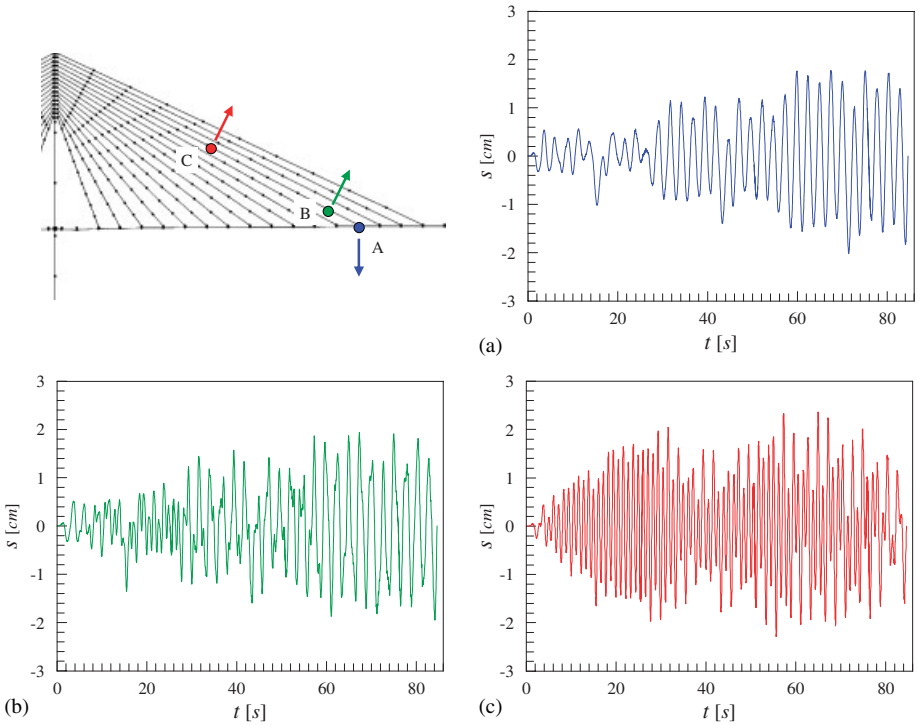

Figure 18. Bridge response to moving load: displacement time history at (a) cable–deck anchorage; (b) measurement point on the cable guide; and (c) cable midspan.

at the measurement point (node B, Figure 18(b)) and at the midspan (node C, Figure 18(c)). The pure dynamic motion has been previously isolated by applying a IIR high-pass filter, which purges the results of the low-frequency quasi-static displacement of the periodic moving load.

The peak displacement values of the cable are about 2.8–3.0 cm (Node B) and of 1.5 cm (Node C), substantially similar to the maximum deck displacement, which is around 3.5–4.0 cm (Node A). It is, however, remarkable that all the oscillation amplitudes have an evident increasing trend, and that a steady state is not still reached at the end of the excitation period (around 63.4 s). Moreover, the cable midspan amplitude exhibits a beating-type behaviour, which could be referred to the interaction of close frequency modes.

Figure 19 shows the FFTs of the displacement time histories. It can be noted that the deck response is dominated by the first bridge global mode M1 ($f_1 = 0.391$ Hz). Differently, the response frequency content of the two cable nodes evidences at least two different peaks, the first one again coinciding with the global mode M1, whereas the second one clearly corresponds to the local mode M72 ($f_{72} = 0.907$ Hz). In particular, the major relevance of the local mode is evident in the cable midspan response, since it represents the node C transform maximum. Simultaneously, in the cable midspan response, a non-negligible participation of the hybrid mode M75 ($f_{75} = 0.951$ Hz) can be recognized, even if the corresponding frequency peak is partially hidden by the closeness of the prevalent local mode. The coupling of these two interacting modes justifies the beating phenomenon already observed in Figure 18.

DOI: 10.1002/stc

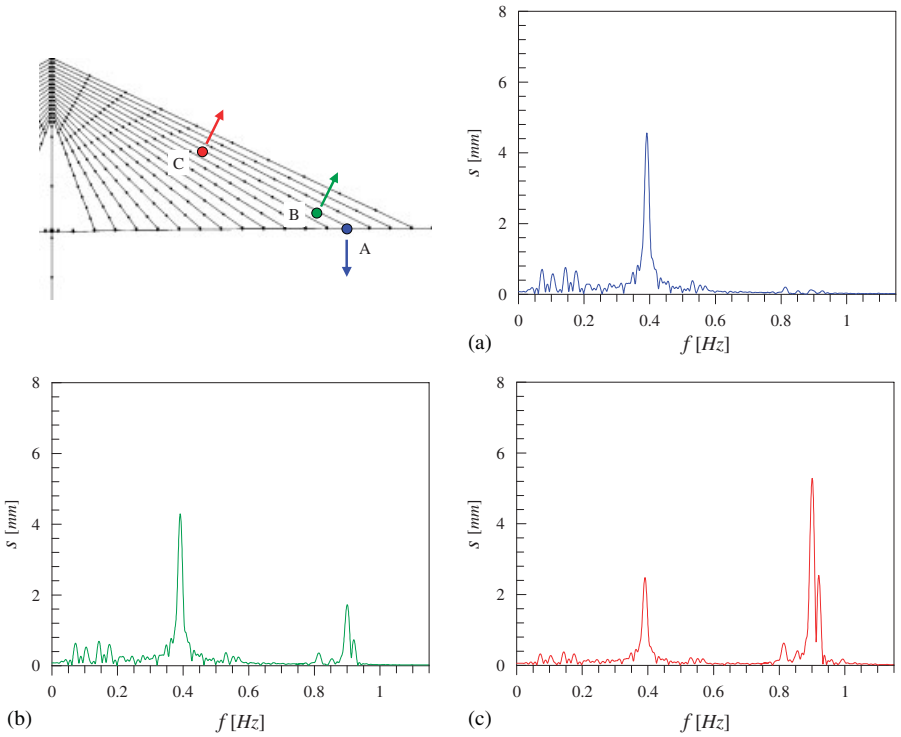

Figure 19. Bridge response to moving load: FFT at (a) cable–deck anchorage; (b) measurement point on the cable guide; and (c) cable midspan.

Based on the FFT of the filtered response, Figure 20 shows the deck and cable midspan peak spectral amplitudes, obtained at the global and the local mode frequencies, versus the moving load velocity. The main remark is that both the peak amplitudes are clearly amplified by velocities ranged between 80 and 90 km/h. Within this range, the greater amplification factor of the cable motion with respect to the deck one is also evident. This effect is partially due to the quasi-static dragging effect of the global mode on the cable, as evident from the ratio of the amplitudes in the nodes B and C at the frequency f_1 (see Figures 20(c)–(e)), and mainly to the local mode, as evident from the same ratio at the frequency f_{72} (see Figures 20(d)–(f)). Finally, it should be noted that in the considered range the amplitude–velocity relation is not strictly monotonic, since for 85 km/h, greater amplification of the global mode is observed, with consequent subtraction of energy to the local mode.

6. CONCLUDING REMARKS

The comprehension of the Guadiana Bridge dynamics involves different challenging aspects, starting from the visual observation of recurrent structural vibrations, followed by their accurate measuring, and finally seeking a reliable interpretation through advanced mechanical models. The correct interpretation of the observed and measured phenomena requires the

DOI: 10.1002/stc

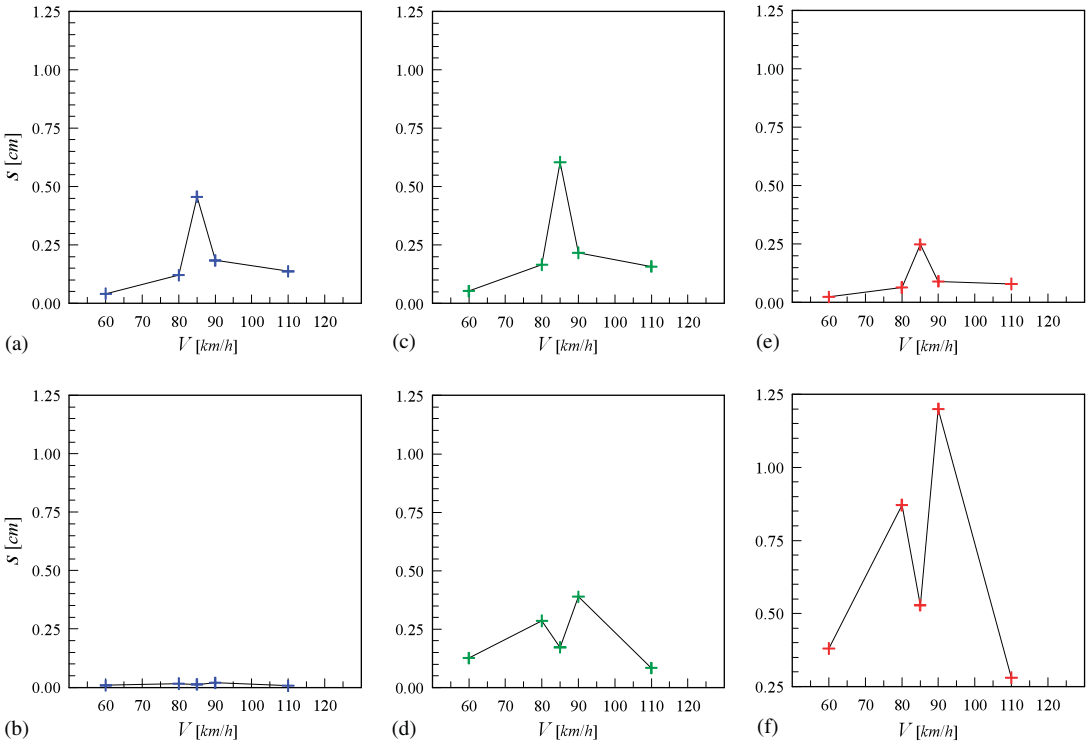

Figure 20. Bridge response versus velocity of the moving load: maximum amplitude at (a) and (b) cable–deck anchorage; (c) and (d) measurement point on the cable guide; and (e) and (f) cable midspan.

comparison of the experimental data with the solution of numerical models able to describe the different dynamic interaction which could involve the cables and the deck under environmental loads, like wind or traffic.

In this work, a three-dimensional FE model of the bridge is developed in order to reproduce with great accuracy the bridge modal properties identified from the dynamic response measured in different testing campaigns. The FE model is obtained through the following improving steps: (a) a preliminary model (OECS) is initially formulated to recognize the global modes of the system, (b) a refined model (MECS) is defined to enhance the description of the transverse cable motion, and (c) an updated model (MECSu) is finally obtained tuning a few mechanical parameters in order to minimize the error between the modal properties identified and those furnished by the finite element description.

The bridge frequency spectrum is deeply analysed to recognize any possible internal resonance that could enable different mechanisms of energy transfer from the global modes of the deck to the local modes of the cables. In particular, the careful classification of all the potential linear and nonlinear coupling evidences that several internal superharmonic and subharmonic resonances may produce high amplitudes of cable oscillations. Nonetheless, the arising of nonlinear phenomena would require quite large deck oscillation amplitudes, which are not consistent with the experimental measures. Differently, the 1:1 resonance condition between local and global modes can produce a strong linear interaction at any amplitude level. This

DOI: 10.1002/stc

resonance is associated with a modal shape distortion, which is here interpreted within the framework of a frequency veering phenomenon and evaluated through a hybridization factor. Furthermore, in the bridge highly dense spectrum, the resonance between a deck frequency and a group of cable frequencies is proved to generate several resonant hybrid modes, which allows the cables to participate in the deck loads.

The bridge response is evaluated under different excitations, selected to approximately simulate the effects of the vehicular traffic. Therefore, random and moving loads are applied on the bridge deck and the linear equations of motion are solved. The solution qualitatively reproduces the localized oscillations observed in a cable pair of the midspan downstream fan, although the vibration amplitude is still not completely sufficient to justify the experimental peaks. On this respect, further improvements of the models and supplementary experimental data are necessary to evaluate, for instance, the effects of simultaneous environmental loads, or even the occurrence of localization phenomena that may arise in nearly periodic structures.

ACKNOWLEDGEMENTS

This work was partially supported under the FY 2004-2005 PRIN Grant 'Vibrations in civil engineering structures' from the Italian Ministry of University and Research and by the Project PCTI/ECM/46475/ 2002 from the Portuguese Science Foundation FCT. Measurements have been performed with authorization from the Portuguese Road Institution EP. The authors deeply acknowledge all the provided support.

REFERENCES

1. Branco F. Special studies for the cable-stayed international Guadiana bridge. In *Proceedings of the International Conference on Cable-stayed Bridges*, Kanok-Nukulchai W (ed.), Bangkok, Thailand, 1987.
2. Branco F, Azevedo J, Proença J. Dynamic testing of the international Guadiana bridge. *CMEST EP Report 35/91*, Lisbon, 1991 (in Portuguese).
3. Branco F, Azevedo J, Ritto Correia M, Campos Costa A. Dynamic analysis of the international Guadiana bridge. *IABSE Structural Engineering International* 1993; **4**:240–244.
4. Bosdogianni A, Olivari D. Wind- and rain-induced oscillations of cables of stayed bridges. *Journal of Wind Engineering and Industrial Aerodynamics* 1996; **64**(2–3):171–185.
5. Warnitchai P, Fujino Y, Susumpow T. A non-linear dynamic model for cables and its application to a cable–structure system. *Journal of Sound and Vibration* 1995; **187**(4):695–712.
6. Perkins NC. Modal interactions in the non-linear response of elastic cables under parametric/external excitation. *International Journal of Non-linear Mechanics* 1992; **27**(2):233–250.
7. Lilien JL, Pinto da Costa A. Vibration amplitudes caused by parametric excitations of cable stayed structures. *Journal of Sound and Vibration* 1994; **174**(1):69–90.
8. Pinto da Costa A, Martins J, Branco F, Lilien JL. Oscillations of bridge stay cables induced by periodic motions of deck and/or towers. *Journal of Engineering Mechanics* 1996; **122**(7):613–622.
9. Gattulli V, Lepidi M. Nonlinear interactions in the planar dynamics of cable-stayed beam. *International Journal of Solids and Structures* 2003; **40**(18):4729–4748.
10. Pinto da Costa A, Branco F, Martins J. Analysis of the cable vibrations at the international Guadiana bridge. *Proceedings of AIPC-FIP International Conference on Cable-stayed and Suspension Bridges*, Deauville, France, 1994.
11. Gattulli V, Lepidi M, Caetano E, Cunha A. Cable–deck dynamic interactions at the international Guadiana bridge. *Proceedings of the 3rd IABMAS International Conference on Bridge Maintenance Safety and Management*, Porto, Portugal, 2006.
12. Caetano E, Cunha A, Taylor CA. Investigation of dynamic cable–deck interaction in a physical model of a cable-stayed bridge: (I) modal analysis, (II) seismic response. *Earthquake Engineering and Structural Dynamics* 2000; **29**(4):481–521.
13. Gattulli V, Lepidi M. Localization and veering in the dynamics of cable-stayed bridges. *Computers and Structures* 2007; **85**(21–22):1661–1678.

DOI: 10.1002/stc

14. Caetano E, Cunha A. Identification of parametric excitation at the international Guadiana bridge. *Proceedings of the 5th International Symposium on Cable Dynamics*, Santa Margherita, Italy, 2003.
15. Caetano E, Cunha A, Magalhães F. Vibration assessment of the international Guadiana bridge. *Proceedings of the 6th EURODYN International Conference on Structural Dynamics*, Paris, France, 2005.
16. Magalhães F, Caetano E, Cunha A. Assessment of dynamic properties of Guadiana cable-stayed bridge based on different output-only identification techniques. *Proceedings of the XXIII International Modal Analysis Conference IMAC*, Saint Louis, U.S.A., 2005.
17. Macdonald J, Daniell W. Variation of modal parameters of a cable-stayed bridge identified from ambient vibration measurements and FE modelling. *Engineering Structures* 2005; **27**(13):1916–1930.
18. Wilson JC, Gravelle W. Modelling of a cable-stayed bridge for dynamic analysis. *Earthquake Engineering and Structural Dynamics* 1991; **20**(4):707–721.
19. Câncio Martins JL. International bridge over the river Guadiana in Castro Marim. *Pontes Atirantadas do Guadiana e do Arade LNEC*, Fernandes, Santos (eds), 1993 (in Portuguese).
20. Ernst JH. Der E-Modul von Seilen unter berucksichtigung des Durchhanges. *Der Bauingenieur* 1965; **40**(2):52–55.
21. Abdel-Ghaffar AM, Khalifa M. Importance of cable vibration in dynamics of cable-stayed bridges. *Journal of Engineering Mechanics* 1991; **117**(11):2571–2589.
22. Nazmy AS, Abdel-Ghaffar AM. Three-dimensional nonlinear static analysis of cable-stayed bridges. *Computers and Structures* 1990; **34**(2):257–271.

DOI: 10.1002/stc